AIAA JOURNAL
Vol. 39, No. 9, September 2001

Analysis of Unsteady Pressure Signals on a Pitching Delta Wing

F. N. Coton,* M. L. Jupp,† and R. B. Green‡
University of Glasgow, Glasgow, Scotland G12 8QQ, United Kingdom

Results from wind-tunnel tests conducted on a pitching 60-deg delta wing in ramp-up motion are presented and described. The wing was instrumented with 192 miniature pressure transducers, which, in conjunction with a powerful multichannel data-logging system, allowed the distribution of time-varying surface pressures to be measured at high temporal resolution for a range of pitching cases. In addition to allowing the forward progression of vortex breakdown with incidence to be tracked, it has been possible to isolate dominant postbreakdown buffet frequencies in both the static and pitching cases. It is demonstrated that, during pitch up, these frequencies differ significantly from those of the static case, indicating that alterations in flow structure may be taking place.

Nomenclature

c = root chord
f = frequency
n = nondimensional frequency $(fx/U)\sin\alpha$
r = reduced pitch rate $(\dot{\alpha}c/2U)$
s = local semispan
U = mean freestream velocity
x = chordwise distance from apex
xb = chordwise distance of vortex breakdown from apex
y = spanwise distance from wing centerline
α = angle of incidence, deg
$\dot{\alpha}$ = pitch rate, rads^{-1}

Introduction

THE flow structures on the leeward surface of sharp-edged delta wings have been the subject of research since the early 1950s. It is now well known that the flow is dominated by a pair of primary vortices extending rearwards from the wing apex. The location and height above the wing of each centerline is chiefly dependent on angle of attack, the sweep angle, and the shape of the leading edge.[1] Each primary vortex is responsible for the formation of a secondary smaller vortex structure rotating in opposition to its primary parent.

As may be expected, the primary vortices dominate the lift response of the wing and allow the generation of lift to continue at angles of incidence beyond the recognized stall condition of conventional wings. However, at some value of incidence and at some point along the vortex core, a sudden transformation takes place causing the axial velocity of the flow to stagnate and the vortex to break down into large-scale turbulence. This phenomenon of vortex breakdown or burst has greatly interested researchers because it was apparently first observed by Peckham and Atkinson[2] in 1957. Experimental research programs in this area[1–4] have made extensive use of flow visualization and qualitative techniques to clarify the physical mechanisms involved in the formation, maintenance, and eventual breakdown of vortical flows.

When a delta wing is subject to pitching motions, the same basic flowfield features exist above the wing, but, inevitably, the manner in which they evolve is influenced by the motion of the wing. Gad-el-Hak and Ho[5,6] demonstrated the strongly hysteretic nature of the position of flowfield structures above the wing and a dependence on reduced frequency in a series of flow-visualization studies in a water tunnel. Similarly, Le May et al.[7] noted that the extent of the hysteresis loop increased with increasing reduced frequency. Others,[8,9] notably Atta and Rockwell,[8] observed a lag in the movement of the vortex breakdown location as the wing was pitched. In some cases the detailed flow structure has been investigated, and valuable insight into the breakdown process has been forthcoming. For example, in the study of Lin and Rockwell,[10] the transient relaxation of the leading-edge vortex after the wing was pitched to high angles of attack was studied using particle image velocimetry. It was found that the vortex breakdown process under these conditions was characterized by a series of abrupt transformations to the structure of the leading-edge vortex and that the phasing of these transformations determined the rate of upstream progression of breakdown.

Numerical studies[11,12] of vortex breakdown on delta wings have also contributed to contemporary understanding of the phenomenon. In relation to pitching wings, the study of Visbal[11] is particularly notable. This study suggested that the pressure gradient along the vortex axis plays a significant role in the initiation of vortex breakdown. Not surprisingly there have also been a number of experimental studies involving the measurement of surface pressures on a series of stationary and pitching wings.[13–17] It has been successfully shown that, in a similar manner to the flowfield, there is consistent hysteretic behavior associated with the pressure distribution on pitching wings when compared with the stationary wing at a given angle of attack. In a similar manner to vortex breakdown, the phase lag in pressure measurements appears to be chiefly dependent on pitch rate. In many cases, however, the studies have been compromised by the limitations of the test setup used. Small numbers of transducers and/or relatively low sampling rates have resulted in low spatial and temporal resolutions, which make vital components of the flow structure difficult to resolve and explain.

This paper describes a series of experiments on a delta-wing planform with sharp leading edges. In these tests, which were carried out in the Handley–Page wind-tunnel facility at Glasgow University, a fully automated data acquisition system was used to obtain unsteady surface-pressure measurements at high temporal and spatial resolution. The high temporal resolution of the measured data allowed a detailed analysis of the fluctuation components of the signals obtained from high-speed pitching cases to be conducted. It is shown that these signals reveal flow features that cannot normally be observed in traditional pressure measurements. It is also demonstrated that this method of analysis can be used to track the forward progression of vortex breakdown with incidence. Finally, it is shown that the dominant frequency of pressure fluctuations in the postbreakdown region is sensitive to pitch rate. This result has implications for buffet on maneuvering aircraft.

Experimental Methods

Model Design and Construction

The delta wing used in the test program was machined from a solid block of aluminum. It had an 800-mm root chord and a sweep angle of 60 deg. This gave an aspect ratio of 2.31 and a trailing-edge span of 923.8 mm. The wing had a flat leeward surface, a highly contoured windward surface (giving a thickness ratio of 9.0%), and beveled edges on the windward side to produce sharp leading and trailing edges. The model was designed to accommodate 192 Kulite

Received 27 April 2000; revision received 27 March 2001; accepted for publication 2 April 2001.

*Reader, Department of Aerospace Engineering. Member AIAA.
†Postgraduate Student, Department of Aerospace Engineering.
‡Lecturer, Department of Aerospace Engineering.

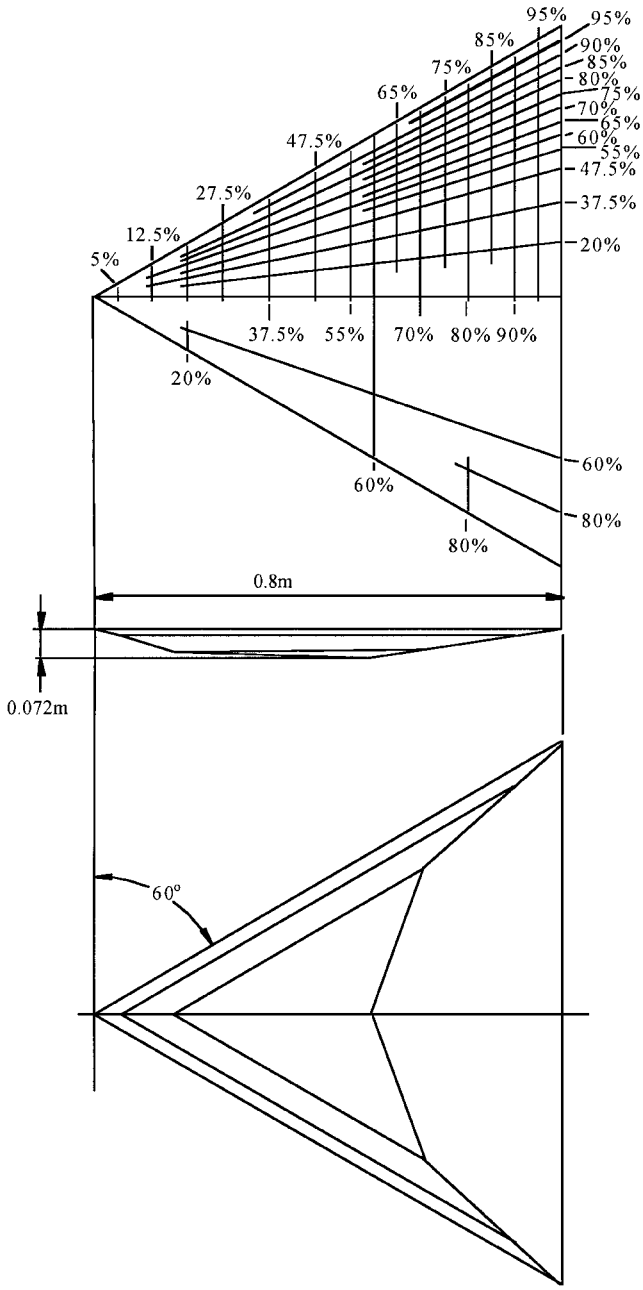

Fig. 1 Delta-wing model leeward surface transducer positions and windward surface shape.

Type CJQH-187 differential pressure transducers located primarily on the starboard side of each surface. The shape of the windward surface and the locations of the leeward surface transducers are shown in Fig. 1.

Wind-Tunnel Facility

The tests were conducted in the department's Handley–Page wind-tunnel facility. This is a closed-return-type wind tunnel with an octagonal test section measuring 2.13 × 1.61 m (working area = 2.667 m^2), which gave a model-span-to-tunnel-width ratio of 43.4% and a model blockage (not including strut fairings) of 1.25–9.27% over the incidence range 0 deg $\leq \alpha \leq$ 42 deg. The model was mounted leeward side up and was supported by three vertical struts mounted on the windward surface, one placed at the quarter-chord position and two at the trailing edge. The forward strut was rigidly fastened to a support structure mounted on the concrete floor below the wind tunnel. The two rear struts were connected to a hydraulic actuation mechanism situated below the tunnel floor.

The model was pitched about the quarter-chord position by vertical displacement of the two rear struts using a Parker 2H Series linear hydraulic actuator. This system used a fast-response proportional-directional control valve with a E200-595 PID analog closed-loop controller, which could deliver a maximum thrust of 17.0 KN during extension and 6.53 KN during retraction at a piston speed of 1.1 m/s. An angular displacement transducer mounted at the pitch location was used to provide the feedback signal, which was also used for recording the instantaneous angle of attack. The required motion profile was provided by an AMSTRAD 1512 microcomputer equipped with an Analog Devices RT1815 multifunction input/output board. The required output function was digitized into equal time steps, and the frequency was controlled using interrupts on the AMSTRAD microcomputer.

Data Acquisition System

Data acquisition was carried out by a PC equipped with a 486 processor, programmed using TEAM 256 software. The PC was configured and interfaced with propriety Bakker Electronics BE256 modules, which provided the necessary analog to digital conversion. The system had 200 channels, each capable of sampling at 50 kHz. The channels not taken up by transducers were used to sample temperature, barometric pressure, reference dynamic pressure, and model incidence. The signals from each transducer were delivered to a specially designed signal conditioning unit of modular construction, and each module contained its own control board. The lowest frequency response of any of the transducer installations was measured to be in excess of 1 kHz, whereas all significant frequencies measured during testing were below 500 Hz.

Experimental Errors

The BE256 data logger and software employ an automatic gain adjustment feature, which allows measurements to be taken at the maximum resolution possible for the system. The system also has an automatic offset removal feature that is used prior to each run to remove potential errors from electronic drift. On the basis of previous experience[18] with the Kulite miniature transducers and taking account of transducer nonlinearity (0.2%), data acquisition system resolution (12 bit), dynamic pressure measurement accuracy, and calibration factor errors, the uncertainty in the measured pressure coefficient was estimated to be 0.5%. The uncertainty in instantaneous incidence was less than 0.25 deg from the angular displacement transducer and the nonlinearity in the reduced pitch rate during the linear portion of the ramp motion was better than 0.5%.

Experimental Procedure

For each of the ramp tests, the wing was set at a starting incidence of −5 deg and pitched up at a constant pitch rate over an arc of 45 deg. Some 8000 samples of pressure data were collected during each cycle, and the ramp motion was repeated over several cycles. Data from four cycles of motion were recorded at each pitch rate to give a total of 32,000 samples over the range of incidence under consideration. The data were not corrected for blockage effects. The mean freestream velocity for all tests was measured at 50 ms^{-1}, which gave a Mach number of 0.162 and a Reynolds number of 2.7×10^6 based on root chord.

Results and Discussion

Static Tests: Mean Pressure Distributions

A full description of a series of static tests conducted on the present delta wing is given in Jupp et al.[19]; however, the following is a brief summary of the results from these tests to provide a benchmark against which significant features observed in the pitch-up cases can be examined and compared. Many previous studies have reported the general form of the upper surface pressure distribution, which is characterized by a suction ridge extending from the apex of the wing toward the trailing edge. This ridge, which is indicative of the primary vortex core location,[16,19] first appeared at around 2-deg incidence at a span location of $(y/s) = 0.7$ in the present case. For all angles of incidence, the magnitude and localization of the suction ridge were at a maximum at the apex of the wing, with a decrease in magnitude and a broadening of the ridge toward the trailing edge. Similarly, the suction magnitude tended to increase and move inboard as the wing incidence was increased.

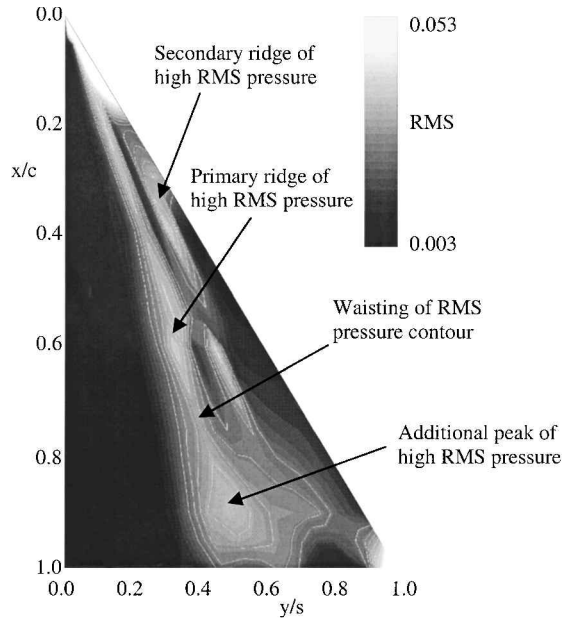

Fig. 2 Contour plot of the upper-surface rms pressure distribution in the static case at an incidence of 13 deg.

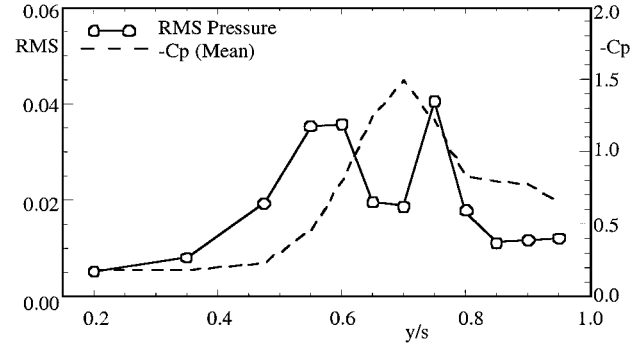

Fig. 3 Spanwise rms and mean-pressure distributions in the static case at chord station $x/c = 0.6$ at an incidence of 10 deg.

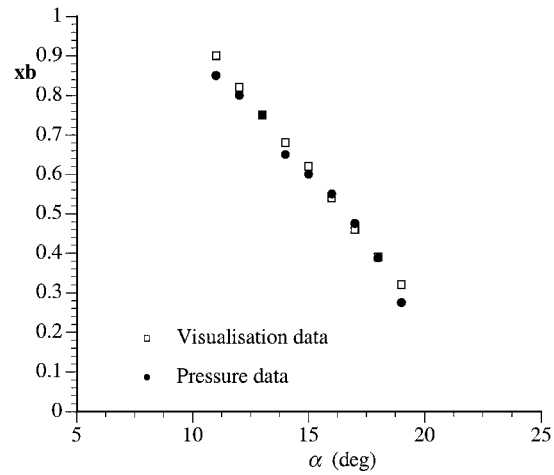

Fig. 4 Position of vortex breakdown against incidence as determined from flow visualization and pressure analysis in the static case.

Static Tests: RMS Pressure Distributions

To obtain more insight into the flow behavior than the mean pressure coefficient distribution could provide, the rms pressure fluctuations around the mean were examined over a range of incidence in Ref. 19. Figure 2 shows the rms pressure distribution at a moderate incidence of 13 deg. The general features identified in this diagram are typical of those observed across the range of incidence, albeit the distribution of the features varies with incidence. Examination of the distribution shows the growth of a primary ridge of high rms pressure along a ray from the apex toward the trailing edge. Like the mean pressure coefficient distribution, this ridge grows in strength with an increase in incidence, but unlike the mean pressure coefficient distribution its strength does not diminish with distance from the wing apex. At low incidence this ridge is the only significant feature in the rms distribution, but, as the incidence is increased, the ridge splits in two as the secondary ridge identified in the figure develops outboard of the primary. Initially, this secondary ridge almost extends continuously to the trailing edge, but, at around 12-deg incidence, it begins to fragment as shown. More significantly, an additional peak of high rms pressure forms and expands on the primary ridge at a point close to the trailing edge as shown in the figure. With further increases in incidence, this additional rms peak continues to expand and move toward the apex of the wing. The significant features accompanying the appearance of the additional peak are a "waisting" of the primary ridge upstream of the peak center followed by a significant expansion toward the peak. The narrowest part of the waist corresponds to the minimum in a small localized trough of rms pressure, which occurs before the rapid increase toward the peak. A detailed discussion of the physical significance of the behavior just identified is provided by Jupp et al.[19]

Figure 3 shows the rms pressure distribution across the span of the wing at a chord station of $x/c = 0.6$ at an incidence of 10 deg. Also plotted is the corresponding mean negative pressure coefficient distribution. It is clear from this plot that the primary region of high rms pressure lies inboard of the centerline of the primary vortex core. The secondary rms pressure region, when apparent, lies outboard of the core. This plot is typical of the rms pressure distribution measured at chordal positions ahead of vortex breakdown. Similar results were observed by Woods and Wood[20] in their work on novel wing planforms and can also be deduced from the flowfield measurements of Payne et al.[21]

Previous work[22] utilizing off-body velocity measurements at moderate incidence identified a region of high turbulent kinetic energy above the surface of the wing inboard of the primary vortex core but outboard of the primary attachment zone. Similarly, two smaller regions of similar energy intensity were measured in areas that correspond to the separation and reattachment zones of the secondary vortex. It is therefore likely that the primary region of high rms pressure observed inboard of the vortex core is associated with a region of localized but highly turbulent flow within the feeding vortex sheet between the vortex core and the primary attachment region. Similarly, it is thought that the secondary region of high rms pressures observed outboard of the vortex core is somehow associated with the formation of the secondary vortex structure.

Static Tests: Progression of Vortex Breakdown

The forward progression of vortex breakdown with incidence observed in a series of smoke flow visualization tests[23] is presented in Fig. 4. These tests were conducted in a smaller wind tunnel on a smaller but otherwise identical delta wing at a Reynolds number of 1×10^4 based on the root chord. Previous work has documented that the location of vortex breakdown is relatively insensitive to Reynolds number[24] provided that the geometry of the model and test environment is consistent between two tests. The size of the smaller model was chosen such that the span-to-tunnel-width ratio was the same as in the pressure measurement tests. Full details of the smoke flow visualization tests are provided in Refs. 19 and 23.

Also plotted in Fig. 4 is the variation with incidence of the chordwise location of the apex of the expanded region of high rms pressure that develops on the primary ridge. Determination of this apex is, to some extent, sensitive to the number of contour levels plotted but can generally be determined with confidence to within 3% of chord. By comparing the two sets of results, it can be seen that there is good agreement, confirming that a relationship exists between the appearance and subsequent movement of the additional peak of high rms pressure and the vortex breakdown phenomenon.

Pitch-Up Motion: Instantaneous Pressure Distributions

In the pitching cases each sample of collected pressure data was nondimensionalizedand point averaged over the four cycles to produce values of instantaneouspressure coefficient. The instantaneous pressure coefficient data again revealed basically the same features as in the static case. This time the suction ridge originated on the leading edge of the wing just downstream of the apex and extended toward the trailing edge. It first became apparent in pitch-up cases at an incidence of approximately 2 deg. As the incidence reached 4 deg, the origin of the suction ridge began to move upstream, reaching the apex at 8 deg. In the pitch-up cases over the incidence range of 2–11 deg, the suction region tended to be narrower and have a lower magnitude, the higher the pitch rate. For all incidences above 11 deg, however, the suction region exhibited a progressive "lag" in the loss of magnitude of the suction region toward the trailing edge, the higher the pitch rate.

Pitch-Up Motion: RMS Pressure Distributions

The high temporal resolution of the data provided the opportunity to study the rms pressure distributions of the pitching cases. This was done over a small incidence range rather than at single points because of limitations in the volume of data recorded. The method involved identifying an incidence range, or window, within which the rms would be calculated. To minimize "smearing" of results across an incidence range, that is to say, mixing pre- and postbreakdown data, the incidence window had to be kept as small as possible. There was, however, a limit to the size that a given incidence window could be minimized to. This was determined by the pitch rate and the pressure fluctuation frequency of interest. The higher the pitch rate, the smaller the time period spanning a given incidence range. Therefore, increasing the pitch rate increases the lower limit of frequency of pressure fluctuations that satisfy the Nyquist criterion. Examination of the frequency power spectra of pressure fluctuations on the pitching wing at reduced pitch rates of $r = 0.007$ (55 deg/s) and $r = 0.015$ (115 deg/s) revealed a band of frequencies, whose appearance and dominance in the static case had been shown to be associated with the onset and progression of vortex breakdown.[19,20,25,26] To capture these frequencies in their entirety, it was necessary to set the incidence windows to 1.5 and 2.0 deg, respectively.

Once the size of the incidence window had been established, the window was applied around the nominal incidence being studied. The windowed data from each of the four measurement cycles were then combined into one data set of approximately 1400 samples per transducer through which a linear best-fit trend line was obtained. The rms values were then calculated about this trend line for each measurement location. RMS values obtained in this manner can only be considered as an approximation to the true rms, and, on the basis of the preceding discussion, low-frequency components within the data cannot be detected. The accuracy of the rms and frequency components obtained by the windowing approach could be estimated at a given incidence by direct comparison of the technique with values obtained by long-duration sampling at the given incidence. In the static case up to 32,000 samples were recorded for each transducer at each incidence value over a 2-s period and so direct comparison could be made. In addition, the effect of applying the window over a range of incidence could also be estimated on the basis of the static data. On this basis the uncertainty in the rms value introduced by the use of the windowing method was estimated to be 3%.

Figure 5 shows the rms pressure distributions on the leeward surface of the wing at three incidence values during pitch up at $r = 0.015$. At an incidence of 8 deg (Fig. 5a), the ridge of high rms pressure located along a ray from the apex toward the trailing edge is well-established. The initial appearance of this ridge in the pitch-up cases occurred at an incidence of 1 deg. By 8 deg the region of high rms can again be seen to be split into two. The primary region extends from the apex to the trailing edge, whereas the secondary region, which forms as incidence is increased, is seen as a branch of the primary emanating downstream of the apex and terminating short of the trailing edge. The similarity in behavior of both these ridges of high rms pressure with their counterparts in the static case

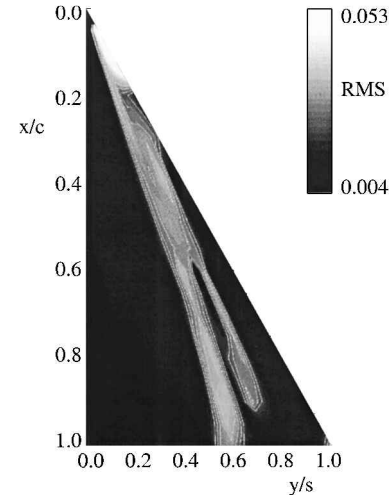

Fig. 5a RMS pressure contours at 8-deg incidence during ramp motion ($r = 0.015$).

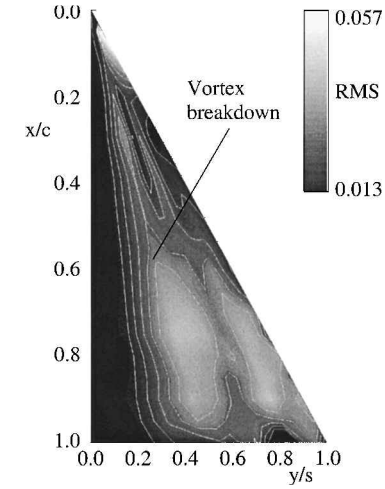

Fig. 5b RMS pressure contours at 19-deg incidence during ramp motion ($r = 0.015$).

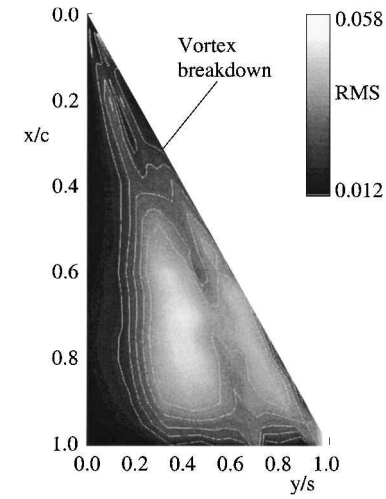

Fig. 5c RMS pressure contours at 24-deg incidence during pitch-up motion ($r = 0.015$).

would suggest that these two features are again associated with the primary and secondary vortex structures in the manner already described.

Figure 5b shows the rms pressure distribution at an incidence of 19 deg. It can be seen that the secondary branch of high rms pressure shown in Fig. 5a is still apparent. Significantly in the $r = 0.015$ case, the additional peak of high rms pressure associated with vortex breakdown is well formed on the ridge of the primary ridge aft of

the 60% of root chord location. Careful scrutiny of all data revealed that the additional peak first appeared at the trailing edge for the $r = 0.007$ and the $r = 0.015$ cases at 13 and 15 deg, respectively. The significant features accompanying the appearance of this feature are again a waisting of the just-described primary ridge of high rms pressure upstream of the peak center, followed by a significant expansion toward the peak in a similar manner to the static case. The narrowest part of the waist corresponds to the minimum in a small localized trough of rms pressure, which occurs before the rapid increase toward the peak. For the pitch-up cases the forward progression of these features always lags the static case progressively with increasing pitch rate. The forward progression with incidence can be observed by comparison of Fig. 5b with Fig. 5c, where the incidence has increased to 24 deg. In each case the perceived location of vortex breakdown is identified in the figure.

Pitch-Up Motion: Progression of Vortex Breakdown

In a manner consistent with the preceding information, the smoke flow visualization tests showed that the appearance of vortex breakdown over the trailing edge and its subsequent progression upstream toward the wing apex were subject to an increasing delay or lag with increase in pitch rate. The observed chordwise progression of vortex breakdown is presented in Fig. 6. Also plotted on the same axes is the corresponding variation with incidence of the chordwise location of the apex of the expanded region of high rms pressure. By comparing each of the two sets of results, it can be seen that there is again good agreement, suggesting that it is possible to track vortex breakdown in pitch-up cases using the unsteady pressure signals.

Postbreakdown Frequency Analysis

Previous work by Gursul[25] demonstrated that once breakdown has progressed forward of a given point on the wing the pressure signal there is dominated by a characteristic frequency. It is likely that this frequency is associated with the helical mode instability of the vortex breakdown flowfield. Despite extensive analysis of postbreakdown dominant buffet frequencies on static wings,[19,20,25,26] it is apparent that until now no data are available regarding this dominant frequency in the pitching case. The power spectrum of the sampled pressure data for each incidence window was calculated for 42 pressure transducers. In each case the data were filtered using a finite impulse response high-pass digital filter to remove spectrum

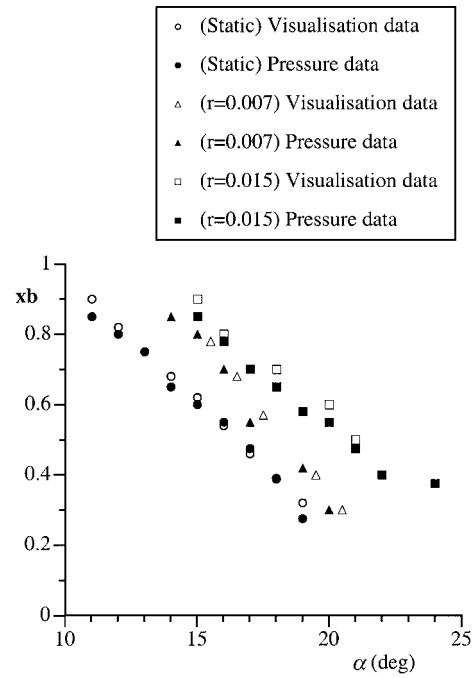

Fig. 6 Position of vortex breakdown against incidence as determined from flow visualization and pressure analysis in the static and two pitching cases.

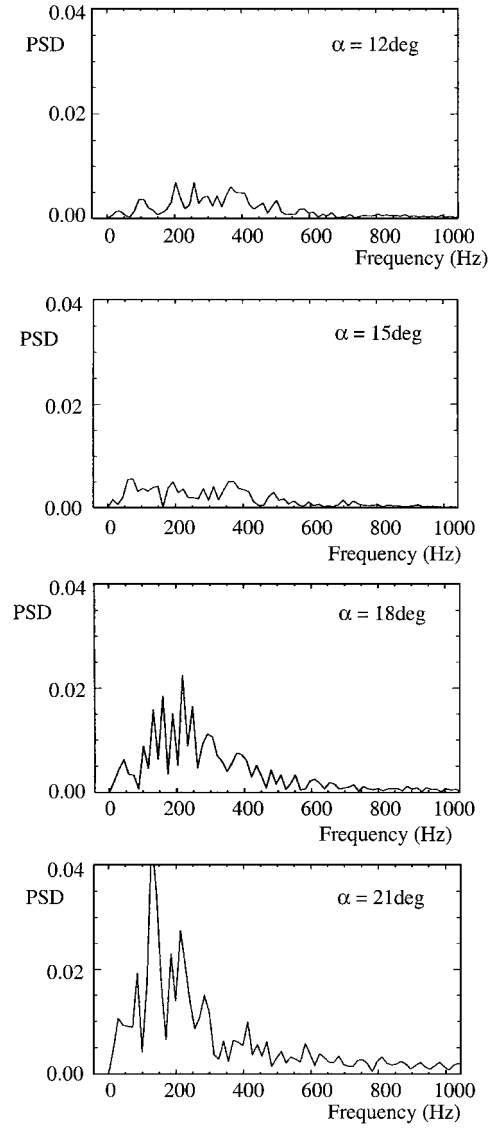

Fig. 7 Pressure frequency power spectra for a transducer located at $x/c = 0.6$, $y/s = 0.6$ at four angles of incidence for the pitch-up case $r = 0.007$.

data below the pitch rate Nyquist cutoff frequency. The transducers chosen were those identified by the earlier analyses as being located under the path of the vortex core centerline and in the region of high rms pressure inboard of the vortex core. A series of power spectra are shown in Fig. 7 for the transducer located at $x/c = 0.6$; $y/s = 0.6$. The figure shows the power spectra at four angles of incidence (12, 15, 18, and 21 deg) for the pitch-up case $r = 0.007$. At an incidence of 18 deg, a band of frequencies centered around 210 Hz begins to feature significantly in the spectrum. By 21 deg this high-frequency band has come to dominate the frequency spectrum. This feature appears progressively later, closer to the apex in a manner consistent with the forward movement of breakdown.

For static cases[19,20,25,26] the center of the high-frequency band has been found to occur at a higher frequency toward the apex of the wing. Analysis of the center frequency of the high-frequency band in the pitch-up cases would appear to show a similar trend. Figure 8a shows the variation in this parameter against chord position (x/c) at an incidence of 18 deg for all cases examined. The general trend apparent in the data would suggest that the rate of increase in central frequency from trailing edge to apex is lower in the pitch-up cases than for the same transducers in the static case, but the magnitude of the frequency is higher. It has also been shown[19,25] that for a given transducer in the static case the central frequency would tend to decrease with an increase in incidence. Figure 8b shows the variation in the center frequency against incidence at a chord location of

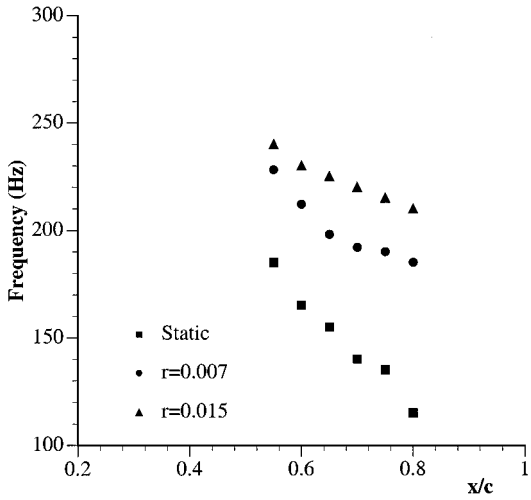

Fig. 8a Postbreakdown buffet center frequency plotted against transducer location at an incidence of 18 deg.

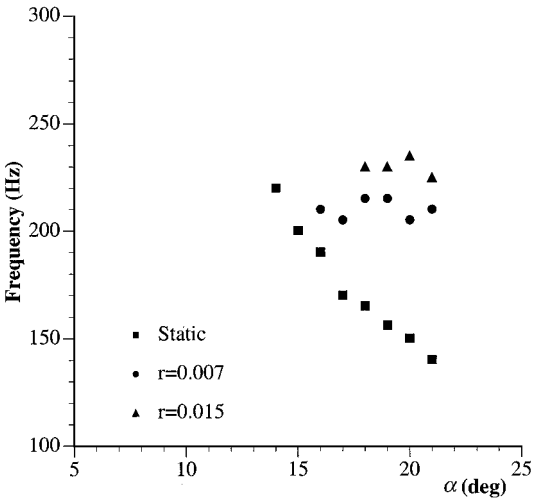

Fig. 8b Postbreakdown buffet center frequency plotted against incidence for a transducer located at *x/c* = 0.6, *y/s* = 0.6.

$x/c = 0.6$. This result is typical of the pitch-up cases studied and quite different from the static case in that the frequency exhibits no obvious incidence dependence.

It is possible that frequency spectra, obtained for chord locations from apex to trailing edge at a given incidence or alternatively obtained at fixed pressure measurement locations over a range of increasing incidence, are actually dissimilar sets of data. In the first case this is because the measurement location is moving downstream away from a stationary breakdown location. In the latter the distance between breakdown location and measurement point is increasing because of the upstream movement of the vortex breakdown location. The following analysis tests this hypothesis by examining the variation in excitation frequencies at a fixed distance downstream of vortex breakdown.

Figure 9 presents a series of plots that show the central frequency in the excitation band of pressure fluctuations for pressure measurement points located a fixed distance downstream of the point of vortex breakdown as incidence is increased in the static case. The nominal fixed distances chosen were $0.1c$, $0.2c$, $0.3c$ behind breakdown. Where the transducer arrangement on the wing precluded the calculation of the frequency spectra at the precise distance behind breakdown, then the next transducer downstream was used instead. Using this criterion, a given fixed distance can be increased by up to $0.0125c$. The actual measurement locations used are shown in Fig. 9a. Figure 9b shows the variation of dominant frequency with incidence, in the static case, at three fixed distances downstream of breakdown. The figure indicates that there is a decrease in excitation

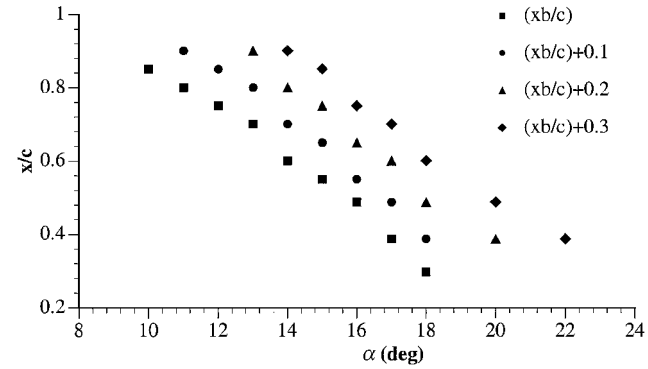

Fig. 9a Measurement locations used in Fig. 9b.

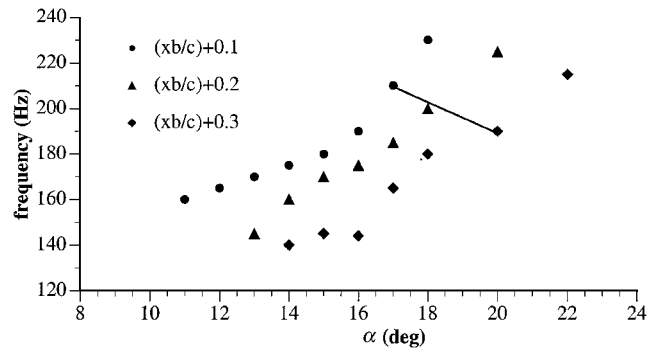

Fig. 9b Frequency downstream of vortex breakdown as a function of incidence in the static case.

frequency values at a given incidence with an increase in fixed distance behind the vortex breakdown location. The line drawn on the figure connects three values obtained at the same location and, once again, illustrates the drop in frequency at a fixed location on the wing with increasing incidence. From this figure it is clear that the dominant frequency just behind vortex breakdown increases as breakdown moves toward the apex of the wing. Subsequently, however, this frequency reduces with downstream distance from the breakdown location. The tradeoff between these two phenomena is responsible for the apparent decrease in frequency at a fixed point on the wing as incidence is increased.

A similar fixed distance frequency analysis was carried out for the two pitch-up cases, $r = 0.007$ and 0.015. The results revealed similar trends to those observed in the static case, indicating that the frequencies of pressure fluctuations in the pitch-up cases also show a strong dependency on vortex breakdown location and downstream measurement location distance. It is interesting, however, to relate these results to those presented in Fig. 8b, where it was observed that at a fixed location on the wing the dominant frequency in the pitching case was independent of incidence. This result suggests that the balance between the increase in frequency just aft of the breakdown location caused by the forward movement of breakdown and its subsequent downstream decay is somehow altered when the wing is pitched.

It has been shown by Mabey[26] that, when expressed in nondimensional terms as $n = (fx/U)\sin\alpha$, the dominant postbreakdown frequency in the static case is more or less a constant for a given geometry and angle of attack. Jupp et al.[19] showed the successful application of this hypothesis to the static 60-deg delta wing described here. Analysis of the present data in a similar manner provides further insight into the behavioral characteristics of the flow over the pitching delta wing.

The frequency data presented in Fig. 8 are shown again in Fig. 10 but this time in nondimensional form. In Fig. 10a the nondimensional frequency at various chord locations on the wing are plotted for a constant incidence of 18 deg. As expected, the static values are approximately constant along the chord. In clear contrast the nondimensional frequency in the pitching case increases with distance from the wing apex. The dominant frequency in the breakdown

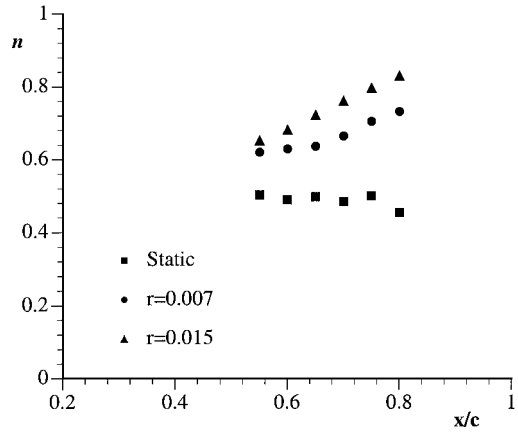

Fig. 10a Nondimensional postbreakdown buffet center frequency plotted against transducer location at an incidence of 18 deg.

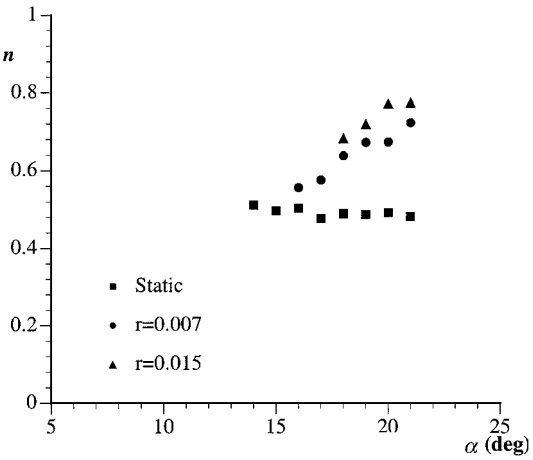

Fig. 10b Nondimensional postbreakdown buffet center frequency plotted against incidence for a transducer located at $x/c = 0.6$, $y/s = 0.6$.

region can been attributed to disturbances rotating in the vortex core. Gursul showed that these disturbances are, in fact, helical waves whose wavelength increases linearly with x. This is consistent with previous observations[27] that the time-averaged flowfield in the breakdown region is conical. The results for the two pitching cases are significantly different from the static case with the nondimensional frequency increasing with distance from the apex. In addition, the rate of increase appears to depend on reduced pitch rate.

Figure 10b shows the variation in nondimensional frequency with angle of incidence at a fixed location on the wing for the static and two pitching cases. Once again the values in the static case are almost constant, whereas in both pitching cases the nondimensional frequency values increase with incidence. Flow visualization has shown that the vortex core radius at any fixed point on the wing increases with angle of attack in the static case. Similarly, the circulation strength also increases with angle of attack. The net effect, however, is that the dimensional frequency reduces with incidence in the manner shown in Fig. 8b.

It is clear from the results presented in Figs. 10a and 10b that the pitching motion of the wing has a strong and consistent influence on the frequency of disturbances in the postbreakdown region. It has been previously observed[5,23] that the vortex core lies closer to the wing surface during pitch-up movement than it does in the corresponding static case. The precise reason for this is unclear, but a contributory factor will inevitably be the pitching velocity across the leading edge that increases with downstream distance from the pitching axis. It is also possible that there is a lag in the response of the leading-edge vortex to the changing incidence. The closer proximity of the vortex to the wing surface during the pitching motion manifests itself in the pressure data as an increase in suction

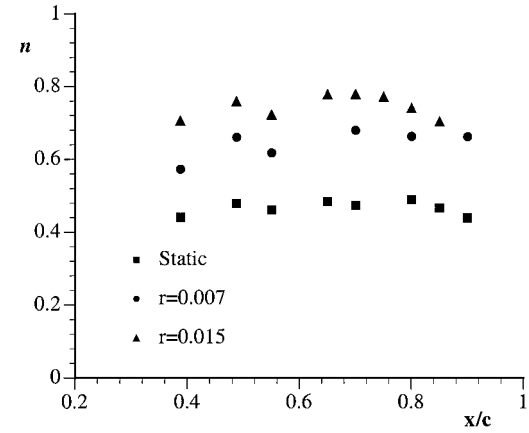

Fig. 11 Nondimensional postbreakdown buffet center frequency at 0.1c downstream of vortex breakdown plotted against chord position.

magnitude near the trailing edge at a given incidence. As shown by Visser and Nelson,[28] the closer proximity of the vortex core to the wing surface will bring faster moving fluid in contact with the wing surface, potentially inducing an increase in the frequency of disturbances. This may provide a partial explanation for an increase in pressure fluctuation frequency.

Further insight into the behavior of the dominant frequency can be gleaned from Fig. 11, which presents the nondimensional frequency measurements 0.1c downstream of breakdown in the static and pitch-up cases. Once again, the nondimensional frequency in the static case is almost constant regardless of the measurement position. Interestingly, in this case the nondimensional frequencies associated with the two pitching cases are also almost constant, albeit at higher levels. Given the proximity of the measurements to the breakdown location, this may suggest that the pitching motion does not destroy the conical nature of the prebreakdown flow in the leading-edge vortex. On the basis of Fig. 10, however, it appears that shortly after breakdown this is no longer the case, and the conical structure of the flow becomes distorted under the influence the pitching motion. Clearly the significant difference between the static and pitching results can have significant implications for the estimation of buffet on maneuvering aircraft, and so a fuller understanding of their origins is clearly desirable. It is likely, however, that a full explanation of this behavior may only be forthcoming when the pressure data are supplemented by comprehensive flowfield measurements.

Conclusions

Experiments to measure the upper-surface-pressure distribution on a pitching 60-deg delta wing with sharp leading edges have been carried out. It has been demonstrated that the high spatial and temporal resolution of the data has, via analysis of the unsteady pressures, facilitated identification of key features of the flow. In addition to allowing the forward progression of vortex breakdown with incidence to be tracked, it has been possible to isolate dominant postbreakdown buffet frequencies. These have been found to be considerably higher than their static counterparts. When nondimensionalized, these frequencies are shown to follow progressive trends with pitch rate, incidence, and downstream distance. It is suggested that the results may indicate departure from the classical conical structure of the leading-edge vortex in the postbreakdown region during pitching. The results also suggest that the use of static data for buffet estimation on maneuvering aircraft may be inappropriate.

Acknowledgments

The wind-tunnel tests reported in this study were carried out with funding from the Engineering and Physical Sciences Research Council (EPSRC), GKN Westland Helicopters Ltd., the Defence Evaluation and Research Agency (DERA), and Glasgow University under Contract GR/H48330. The authors also wish to acknowledge the additional support of the EPSRC through RS Quota Award 96300150. Finally, the authors are indebted to R. Galbraith of the Department of Aerospace Engineering at the University of Glasgow for his continual support and encouragement throughout this project.

References

[1]Lambourne, N. C., and Bryer, D. W., "The Bursting of Leading-Edge Vortices—Some Observations and Discussion of the Phenomenon," Aeronautical Research Council, R&M 3282, London, April 1961.

[2]Peckham, D. H., and Atkinson, S. A., "Preliminary Results of Low Speed Wind Tunnel Tests on a Gothic Wing of Aspect Ratio 1.0," Aeronautical Research Council, TR C.P. 508, London, April 1957.

[3]Gad-el-Hak, M., and Blackwelder, R. F., "Control of the Discrete Vortices from a Delta Wing," *AIAA Journal*, Vol. 25, No. 8, 1987, pp. 1042–1049.

[4]Payne, F. M., Ng, T. T., and Nelson, R. C., "Visualisation and Flow Surveys of the Leading-Edge Vortex Structure on Delta Wing Planforms," AIAA Paper 86-0330, Jan. 1986.

[5]Gad-el-Hak, M., and Ho, C. M., "The Pitching Delta Wing," *AIAA Journal*, Vol. 23, No. 11, 1985, pp. 1660–1665.

[6]Gad-el-Hak, M., and Ho, C. M., "Unsteady Vortical Flow Around Three-Dimensional Lifting Surfaces," *AIAA Journal*, Vol. 24, No. 5, 1986, pp. 713–721.

[7]LeMay, S. P., Batill, S. M., and Nelson, R. C., "Vortex Dynamics on a Pitching Delta Wing," *Journal of Aircraft*, Vol. 27, No. 2, 1990, pp. 131–138.

[8]Atta, R., and Rockwell, D., "Hysteresis of Vortex Development and Breakdown on an Oscillating Delta Wing," *AIAA Journal*, Vol. 25, No. 11, 1987, pp. 1512, 1513.

[9]Jarrah, M. A. M., "Low Speed Wind-Tunnel Investigation of Flow About Delta Wings, Oscillating in Pitch to Very High Angle of Attack," AIAA Paper 89-0295, Jan. 1989.

[10]Lin, J. C., and Rockwell, D., "Transient Structure of Vortex Breakdown on a Delta Wing," *AIAA Journal*, Vol. 33, No. 1, 1995, pp. 6–12.

[11]Visbal, M. R., "Onset of Vortex Breakdown Above a Pitching Delta Wing," *AIAA Journal*, Vol. 32, No. 8, 1994, pp. 1568–1575.

[12]Kandil, O. A., and Chuang, H. A., "Computation of Vortex Dominated Flow for a Delta Wing Undergoing Pitching Oscillation," *AIAA Journal*, Vol. 28, No. 9, 1990, pp. 1589–1595.

[13]Miau, J. J., Chang, R. C., Chou, J. H., and Lin, C. K., "Non-Uniform Motion of Leading-Edge Vortex Breakdown on Ramp-Pitching Delta Wings," *AIAA Journal*, Vol. 30, No. 7, 1992, pp. 1691–1702.

[14]Gursul, I., and Yang, H., "Vortex Breakdown over a Pitching Delta Wing," *Journal of Fluids and Structures*, Vol. 9, 1995, pp. 571–583.

[15]Rediniotis, O. K., Klute, S. M., Hoang, N. T., and Telionis, D. P., "Dynamic Pitch up of a Delta Wing," *AIAA Journal*, Vol. 32, No. 4, 1994, pp. 716–725.

[16]Thompson, S. A., Batill, S. M., and Nelson, R. C., "Delta Wing Surface Pressures for High Angle of Attack Maneuvers," AIAA Paper 90-2813, Aug. 1990.

[17]Thompson, S. A., and Nelson, R. C., "Wind Tunnel Blockage Effects on Slender Wings Undergoing Large Amplitude Motions," AIAA Paper 92-3926, July 1992.

[18]Masson, C., Green, R. B., Galbraith, R. A. McD., and Coton, F. N., "Experimental Investigation of a Loaded Rotor Blade's Interaction with a Single Vortex," *The Aeronautical Journal*, Vol. 102, No. 1018, 1998, pp. 451–457.

[19]Jupp, M. L., Coton, F. N., and Green, R. B., "A Statistical Analysis of the Surface Pressure Distribution on a Delta Wing," *The Aeronautical Journal*, Vol. 103, No. 1025, 1999, pp. 349–357.

[20]Woods, M., and Wood, N. J., "Unsteady Aerodynamic Phenomena on Novel Wing Planforms," *Proceedings of the International Congress of the Aerospace Sciences*, Vol. 2, AIAA, Reston, VA, 1996, pp. 2611–2621.

[21]Payne, F. M., Ng, T. T., and Nelson, R. C., "Experimental Study of the Velocity Field on a Delta Wing," AIAA Paper 87-1232, June 1987.

[22]Honkan, A., and Andreopoulous, J., "Instantaneous Three-Dimensional Vorticity Measurements in Vortical Flow over a Delta Wing," *AIAA Journal*, Vol. 35, No. 10, 1997, pp. 1612–1620.

[23]Green, R. B., "A Flow Visualisation Study of a Pitching Delta Wing," Glasgow Univ., Aero. Rept. 9824, Glasgow, Scotland, U.K., June 1998.

[24]Jobe, C. E., "Vortex Breakdown Location over 65° Delta Wings Empiricism and Experiment," AIAA Paper 98-2526, June 1998.

[25]Gursul, I., "Unsteady Flow Phenomena over Delta Wings at High Angle of Attack," *AIAA Journal*, Vol. 32, No. 2, 1994, pp. 225–231.

[26]Mabey, D. G., "Unsteady Vortex Flow Phenomena on Delta Wings at High Angles of Incidence," *Proceedings of the International Congress of the Aerospace Sciences*, Vol. 2, AIAA, Reston, VA, 1996, pp. 1167–1176.

[27]Roos, F. W., and Kegelman, J. T., "Recent Explorations of Leading Edge Vortex Flowfields," NASA High-Angle-of Attack Technology Conf., NASA Langley Research Center, Hampton, VA, Nov. 1990.

[28]Visser, K. D., and Nelson, R. C., "Measurements of Circulation and Vorticity in the Leading Edge Vortex of a Delta Wing," *AIAA Journal*, Vol. 31, No. 1, 1993, pp. 104–111.

A. Plotkin
Associate Editor